New analysis of the v_6 and 2v_3 bands of methyl iodide (CH_3I)

A. Perrin, I. Haykal, F. Kwaba Tchana, L. Manceron, D. Doizi, G. Ducros

New analysis of the v_6 and $2v_3$ bands of methyl iodide (CH_3I)

I. Haykal[a], D. Doizi[a], A. Perrin[b], F. Kwaba. Tchana[b], L. Manceron[c], G. Ducros[d]

[a] *CEA, Saclay (DEN, Département de Physico-chimie), 91191 Gif sur Yvette Cedex, France (e-mails : imane.haykal@cea.fr, denis.doizi@cea.fr).*

[b] *CNRS et Universités Paris Est et Paris 7, Laboratoire Inter-Universitaire des Systèmes Atmosphériques (LISA), 94010 Créteil, France (e-mail: Vincent.Boudon@u-bourgogne.fr).*

[c] *Ligne AILES, Synchrotron SOLEIL, L'Orme des Merisiers, St-Aubin BP48, 91192 Gif-sur-Yvette Cedex, France (e-mail: laurent.manceron@synchrotron-soleil.fr).*

[d] *CEA, Cadarache (CEA, DEN, Département d'Études des Combustibles), 13108 Saint-Paul-lez-Durance cedex, France. (e-mail : gerard.ducros@cea.fr).*

Abstract

A new rovibrational study of the $v_6 = 1$ band of methyl iodide was conducted to obtain a rather complete line list. Therefore, we accomplished a new analysis in line position. The spectrum of this band has been first recorded using the FTIR Bruker HR125 at the AILES beamline of the SOLEIL Synchrotron facility and later with the Bruker FTIR IFS125HR located at the LISA facility in Créteil. The final analysis led to the assignment of about 10000 infrared lines up to J =85 and $|K|$ =20 quantum numbers, 6000 lines of which are due to the ^{127}I nuclear quadrupole coupling hyperfine structure revealed in the spectrum owing to the iodine nuclei. A global fit based on the Watson model of these new infrared data combined with previously assigned microwave lines [1] helped improving the last set of published parameters for this band [2]. The $v_3 = 2$ band was also analysed and around 1500 lines were assigned. Due to the high values of quantum numbers achieved for the $v_6 = 1$ energy levels, it proved to be crucial to take into account an $\alpha(\Delta\ell = \pm1; \Delta K = \pm2)$ and a $C_x(\Delta\ell = \pm1; \Delta K = \pm1)$ types of Coriolis interactions with the levels of $v_3 = 2$ and of $v_2 = 1$ respectively.

Keywords: `methyl iodide` – `CH3I` – `Line List` – `High-resolution Fourier`

Transform spectroscopy – Rovibrational analysis –Watson Model – Line position

1. Introduction

Methyl iodide, (CH_3I) is emitted to the atmosphere by the oceans and photolyzes with a lifetime of the order of a week. It is a source for the ozone destruction in the upper troposphere and in the lower stratosphere [3]. It is as well of nuclear interest. In the case of a sever nuclear accident, the iodine fission products represent the major part of the released radioactivity and are of high concern due to their affinity to the thyroid. Methyl iodide is produced in the primary circuit by the reaction, under ionising radiation, of iodine with the organic coating of the enclosed containment. Because, in the case of an accident, organic iodine is not efficiently trapped on filters, it is crucial to monitor its release into the atmosphere, as an important goal of the nuclear safety and radio-protection. Hence, the present work concentrates on acquiring a database for a future spectroscopic remote sensing detection of methyl iodide.

To our knowledge, there is up to now no infrared detection of this specie in the atmosphere from satellite instrument. The rather strong ν_6 band of CH_3I, located at 892.916 cm^{-1}, which coincides with the 11 μm window of transparency in the atmosphere, could therefore be a good candidate for such detection. In addition it is relatively isolated from the absorption of the atmospheric molecules, especially water, as shown in figure 1. However, there exist no spectroscopic parameters for this molecule in the common access spectroscopic databases HITRAN [1] or GEISA[2]. This work, which deals with the line positions, is the very first contribution to fill this gap.

This molecule is also one of the most intensively studied symmetric top molecules by means of high resolution spectroscopy for both the for the $^{12}CH_3I$ and $^{13}CH_3I$ isotopologues. It has six vibrational modes which are described

[1] http://hitran.org/

[2] http://ether.ipsl.jussieu.fr/etherTypo/?id=950

shortly in Table 1. Methyl iodide is a prolate symmetric top molecule with an equilibrium configuration belonging to the C_{3v} point group. It has nine fundamental modes, three of which, ν_1, ν_2, ν_3, being non-degenerate modes and belong to the A_1 symmetry representation in addition to three degenerate modes ν_4, ν_5, ν_6 having the E symmetry. The infrared spectrum of methyl iodide is dense in the infrared region due to the iodine nuclei which, on one hand, makes of the methyl iodide a heavy molecule with small values of the rotational constants, and on the other hand, complicates the spectrum by the nuclear hyperfine effect which splits each rovibrational level into six sub-levels labelled by the F quantum number. Its rotational spectrum in the ground and in the first excited vibrational states was investigated in detail by microwave [4, 5, 1], and by Doppler -free double resonance techniques [2, 6]. This molecule was also the subject of numerous infrared studies which concern the ν_1 [7], ν_3 [8], ν_4 [9], ν_5 [10], ν_2, ν_5 and ν_3+ν_6 band system, [11], ν_6 [12, 13, 14, 15, 16, 17], and $2\nu_3$[18] bands and several combination bands in the 2800 cm^{-1} spectral region [19]. In this way, vibrational band centers, rotational and coupling constants, together with, eventually, hyperfine parameters could be obtained for the ground state and for several vibrational states of $^{12}CH_3I$ and $^{13}CH_3I$. Indeed, for CH_3I, hyperfine splittings are easily observable in the microwave region, and eventually also in the infrared region,due to the large values of the iodine nuclear quadrupole moment and spin of the iodine nucleus (I=5/2).

As far as the $\nu_6 = 1$ and $\nu_3 = 2$ vibrational states are concerned, the most recent papers differs in strategy from the present one. The analysis of the ν_6 band of $^{12}CH_3I$ performed by Paso and Alanko [16] by Fourier transform technique is, up to now, the most complete one existing in the infrared literature. Indeed, about 4000 transitions of the ν_6 band were identified for lines involving J up to 70 and K up to 18. However, the identification of this band was complicated by the existence of hyperfine structures which are easily observable for rotational transitions involving rather low J values as compared to the K values ($J \leq 2 \times K$). By correcting perturbed lines from their hyperfine structure, they could increase the number of rotational transitions to be included in the fit. During

the energy level calculation, the weak first order Coriolis resonance coupling together the $v_6 = 1$ and $v_3 = 2$ energy levels was accounted for explicitly. One has to mention that this $v_6 = 1 \Leftrightarrow v_3 = 2$ resonance which was also considered during the investigation of the v_6 band for the $^{13}CH_3I$ isotopologue [15] was not accounted for during the investigation of the $2v_3$ overtone band of $^{12}CH_3I$ and $^{13}CH_3I$ performed by Alanko et al. [18]. Later on, a new investigation of the rotational structure of the ground and $v_6 = 1$ vibrational states of $^{12}CH_3I$ was performed using a Doppler free double resonance technique by Carocci et al. [2]. The results of these rotational measurements were combined with a large set of literature data achieved by microwave techniques [20, 21, 4, 22, 23, 1] together with infrared investigations of the v_6 band. In this way a complete set of rotational and of hyperfine (quadrupole experimental rotational frequencies) was obtained both for the ground and the $v_6 = 1$ excited states of $^{12}CH_3I$. However, the existence of a $v_6 = 1 \Leftrightarrow v_3 = 2$ Coriolis resonance was not mentioned and therefore not accounted for explicitly.

Finally, a new investigation of the v_6 band of $^{12}CH_3I$ was performed very recently by Haykal et al. [17]. This new study aimed at testing the C_{3v}TDS package of the XTDS suite of programs [24] and to demonstrate its capabilities [25]. However, this preliminary study involves a rather restricted set of the v_6 transitions as compared to the one used during the investigation of Paso and Alanko [16]. Indeed, as compared to reference [16] the Fourier transform spectrum used during Haykal's study [17]was recorded for a better resolution , but for a (pressure $\times$ path length) product which is about 20% weaker than in the Paso and Alanko's study. In addition, the hyperfine structure was not accounted for, and the corresponding perturbed lines were not considered in the calculation.

The goal of the present work is to generate a set of accurate line positions for the v_6 band of $^{12}CH_3I$. As the existence of a resonance was mentioned previously, the analysis of the $2v_3$ band was performed in parallel. The infrared data delivered during the present analysis were combined with all existing literature data for rotational transitions within the $v_6 = 1$ and $v_3 = 2$ states. The

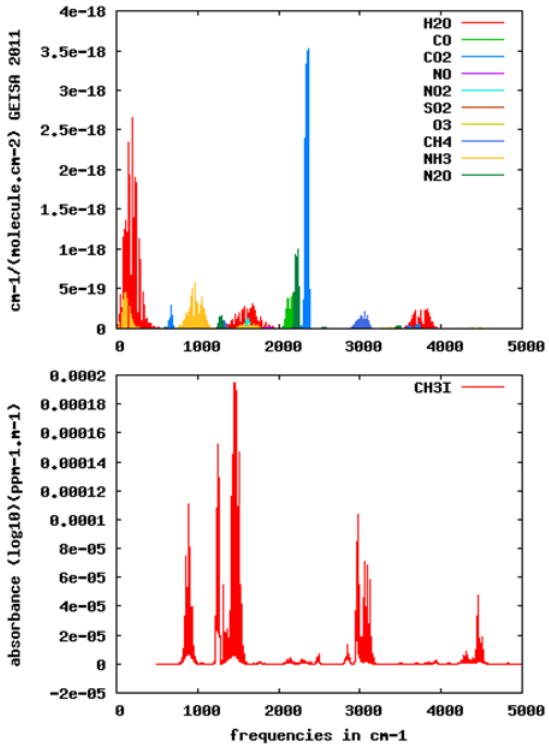

Figure 1: A comparison between a low resolution spectrum of methyl iodide, in red, issued from the PNNL (Pacific Northwest National Laboratory) with another spectrum (the upper spectrum), which combines the GEISA 2011 database for some atmospheric molecules.

theoretical model used during this study accounts for the Coriolis resonances coupling together the $v_6 = 1 \Leftrightarrow v_3 = 2$ energy levels. Surprisingly enough, it proved necessary also to account also for the Coriolis resonance coupling the $v_6 = 1 \Leftrightarrow v_3 = 2$ resonating levels.

Section 2 describes the experimental conditions in which five spectra were recorded. Details on the analysis procedure are listed in section 3 and of the calculations in section 4. Finally, section 5 gives a general conclusion to the present work in addition to some future perspectives. Finally, the theory of the rovibrational Hamiltonian for symmetric molecules presenting a nuclear hyperfine structure effect is recalled in Appendix A.

Table 1: Vibrational fundamental bands of $^{12}CH_3I$

Mode	Symmetry	Description	E_v *	Reference
v_1	A_1	CH_3 stretch	2971.8375	[26]
v_2	A_1	CH_3 deformation	1251.192826	[11]
v_3	A_1	C-I stretch	533.216836	[8]
v_4	E	CH_3 stretch	3060.07890	[9]
v_5	E	CH_3 deformation	1435.013447	[11]
v_6	E	C-I Bending	892.918	[16]
v_6	E	C-I Bending	882.91833100(427)	this work
$2v_3$		Overtone v_3	1059.993378	[18]
$2v_3$		Overtone v_3	1059.99357(1)	this work

* Vibrational energies (E_v) and band center (v) in cm^{-1}.

2. Experimental details

The sample was purchased from Sigma Aldrich (Fluka Chemie GmbH, 99 % purity) and used without further purification. Two absorption spectra of methyl iodide in the mid-infrared spectral region where successively recorded. The first spectrum (spectrum n^o 1) was recorded using the Bruker IFS125HR Fourier transform spectrometer of the AILES beamline at the SOLEIL Synchrotron facility. It presents a high signal to noise ratio thanks to the combination of the synchrotron light and of a new home-made detector developed at the AILES beamline of the synchrotron SOLEIL [27]. A multi-pass cell was use which provided a path length of 4 m. The pressure in the cell was maintained at 0.206 mbar. The spectrum n^o 1 was recorded at room temperature and with a resolution of 0.00102 cm^{-1} (according to the Bruker definition, resolution is 0.9/882 cm, 882 cm being the maximum optical path difference). However, the pressure $\times$ path length (P $\times$ L) was not sufficiently high and a second spectrum (n^o 2) was recorded with the Bruker IFS125HR spectrometer [28] located at the

LISA facility in Créteil at a resolution of 0.0019 cm^{-1}. As for the spectrum n° 1, the home-made detector [27] was implemented. An optical path of 19.249 m was provided by a multi-pass cell. The pressure in the cell was maintained at 0.934 mbar. This spectrum was recorded at 295 K. For both spectra the instrument was equipped with a KBr/Ge beam splitter and an empty cell spectrum was used as the reference. No apodization was applied (Boxcar function in the Bruker software). Peak positions were determined after zerofilling thanks to the Bruker OPUS software using the standard method for well separated peaks and the second derivative for partially overlapping lines.

Figures 2 and 5 represent an overview of the v_6 band of methyl iodide, in the 750 - 1070 cm-1 frequency range, recorded during this study at a low and a high P × L products (Spectrum n° 1 and n° 2, respectively). One can see that the $2v_3$ band is detected for the spectrum n° 2 in the figure 5, while in the case of the spectrum n° 1 in the figure 2, this band is too weak to be observable. Figures 3 and 4 with figures 6 and 7 give detailed views of the spectra n° 1 and n° 2, respectively. It is clear when comparing figures 3 and 4 with the figures (1) and (2) from reference [16], that the high resolution of the spectrum n° 1 provides more information on the hyperfine patterns in comparison to this previous investigation.

3. Rovibrational analysis

According to symmetry considerations for a C_{3v}-type molecule, v_6 is a perpendicular band, while $2v_3$ is a parallel band. The analysis proved to be straightforward in general for the rather unperturbed v_6 and $2v_3$ bands. However, the hyperfine structure which is hardly observable for the $2v_3$ parallel band, is a problem for v_6 transitions involving rather weak values of the J rotational quantum number as compared to K ($J \leq 2 \times K$). Also, for the P branches of each band, lines from several hot bands, like $3\nu_3$-ν_3 centered at 1016.114 cm^{-1} [18] and $\nu_3 + \nu_6 - \nu_3$ at 877.581 cm^{-1} [11], are clearly observable in the spectra which lead, sometimes, to complications in the analysis procedure. The first v_6

and $2v_3$ assignments were performed using the calculated predictions both for line positions and relative line intensities. As the Coriolis resonances perturbing v_6 and $2v_3$ are rather weak, these effects were not accounted for during the preliminary identification process, and the symmetric-top Hamiltonian used for the energy level calculation is described in Appendix A. As usual it includes diagonal z-Coriolis terms together with $(\Delta\ell\ ;\ \Delta K)= (\pm 2;\ \pm 2)$ - type operators for the degenerated $(\ell = 1)$ $v_6 = 1$ state. In addition, the hyperfine structure was considered explicitly and Appendix A details the nuclear quadrupole and the spin-rotation operators which were considered during our calculations. However, in similarity with the references [5] and [1], the $(\Delta J = \pm 1)$ and $(\Delta J = \pm 2)$ matrix elements (see Appendix A) were considered through a second order perturbation treatment.

For the computation of the ground state energy levels we used the rotational and centrifugal distortion constants quoted in reference [2], and this all along the present study. Indeed, the recent ground state rotation constants quoted in table 2 of reference [17] lead to computed ground state combination differences which are in significant disagreement with the observed ones (up to ~ 0.005 cm^{-1} for $J \geq 75$).

For the upper states, the sets of vibrational energies and rotational constants from reference [2, 18] were used as starting values for the calculation of the $v_6 = 1$ and $v_3 = 2$ upper state energies, respectively.

In table 4 are listed the nuclear quadrupole and spin rotational constants originating from Reference [2] and this for the ground and the $v_6 = 1$ vibrational states, as for the $v_3 = 2$ state they were taken from reference [1]. These hyperfine parameters are the ones used along the present study since it proved not to be faithful to refine them. In fact, the present study does not bring any new microwave data detailing the rotational structure in the ground, $v_6 = 1$, or $v_3 = 2$ states. In addition, the relative vibration- rotation intensities were computed using the method described in Reference [29, 30]. More explicitly, the v_6 and $2v_3$ transition moment operators were expanded up to the first order

using the following expressions:

$$^{33}\mu_Z^{\Delta\ell=0} = ^{33}\mu_0^{\Delta\ell=0} \times \Phi_z \tag{1}$$

and;

$$^{6}\mu_Z^{\Delta\ell=0} = ^{6}\mu_0^{\Delta\ell=1} \times \Phi_x \tag{2}$$

Where, Φ_z and Φ_x are the Z_z and Z_x components of the cosines direction respectively between the Z laboratory fixed axis and the z and x molecular axes. The estimated ratio $^{33}\mu_0^{\Delta\ell=0}$ and $^{6}\mu_0^{\Delta\ell=1}$ first order terms are:

$$\frac{^{6}\mu_0^{\Delta\ell=1}}{^{33}\mu_0^{\Delta\ell=0}} \approx 9 \tag{3}$$

In addition, the relative contribution to the intensities of the hyperfine subcomponents were computed using the standard $6j$- method [31, 32].

The assignments of the v_6 and $2v_3$ bands were performed using these predictions and accounting for the perturbations due to the hyperfine structure. As pointed out by Paso and Alanko [16], the individual vibration rotation transitions may be split into different hyperfine subcomponents, or look unsymmetrical or broadened, or, for large J values, be unaffected by such perturbation. This is observable on Figures 5 and 3 where we give, respectively, a detailed views of the band-heads for the $^{P}Q_9$ and $^{R}Q_9$ branches of the v_6 band. So, we adopted the same strategy as the one applied by Paso and Alanko in reference [16]. Thus, two types of assignments were performed during the v_6 and $2v_3$ analyses: For the majority of the v_6 lines and almost all the $2v_3$ transitions, the hyperfine structure is not observable in the infrared. Examples of such "pure vibrational-rotational" transitions are given in the bottom part of Figures 5, 3 and 4. These transitions were included in our list of assignments at their estimated accuracy and without further correction. However a significant portion of the assignments for the v_6 band, and some lines of the $2v_3$ band, are lines for which the effects of hyperfine structure cannot be ignored. In this case, the observed structures correspond usually to clusters of several hyperfine subcomponents. These "hyperfine perturbed transitions" are shifted in position relative

to the corresponding "pure vibration-rotation" lines. These "perturbed lines" were only introduced in our line list after a correction of the calculated hyperfine shift. The uncertainty associated to each of these additional "perturbed" transitions accounts for their relative intensity, in the hyperfine cluster, and for the quality of the associated measured peak position in the Fourier transform spectrum. The final results of the assignments of the ν_6 and the $2\nu_3$ bands are described in table 3. For the ν_6 band (resp. the ν_3 band), the present work represent a significant (resp. reasonable) progress in comparison to the previous infrared investigation [16] (resp. Reference [18]) where the assignments were restricted to J and K values with $J \leq 70$ and to (resp. ($J \leq 70$ and $|K| \leq 12$). The set of the experimental vibrational-rotational energy levels for $\nu_6 = 1$ and for $\nu_3 = 2$ were generated by adding the line positions to the computed ground state energy levels [2]. It is important to mention that when accounting for the lines perturbed by the hyperfine structure in our list of assignments we increased the number of measured rotational energy levels which grows from 1797 (resp. 678) for the and the $\nu_6 = 1$ state (resp. and the $\nu_3 = 2$ state) to 2177 (resp. 692).

Table 2: Statistical analysis of energy level calculation

	ν_6	$2\ \nu_3$
(A)Range of observed energy levels during the analysis of the 12 μm bands of CH_3I:		
Total number of lines*	9248	1495
"Pure vibration-rotation" lines⁎	3976	1370
Max J, K	$J \leq 85, \ell \times K = -19$ to $\ell \times K = +20$	$J \leq 73, \lvert K \rvert \leq 15$
	$v_6 = 1$	v_3 =2
Total number of rotational levels	2177	692
(B) Statistical analysis of the results of the energy level calculation:		
Calculation n°	1▲	2▼
	$(v_3 = 2, \ell = 0)$	$(v_6 = 1, \ell = 1)$
Number of levels	692	2177
$0.0 \leq \delta^{\star} \leq 2 \times 10^{-4} cm^{-1}$	86.2 %	85.2 %
$2 \times 10^{-4} \leq \delta^{\star} \leq 4 \times 10^{-4} cm^{-1}$	11.4 %	11.8 %
$4 \times 10^{-4} \leq \delta^{\star} \leq 7 \times 10^{-4} cm^{-1}$	2.4 %	2.8 %
$8 \times 10^{-4} \leq \delta^{\star} \leq 1.8 \times 10^{-3} cm^{-1}$		0.2 %
Standard deviation (in cm^{-1})	0.12×10^{-3}	0.17×10^{-3}
Calculation n°	3♦	
	$(v_3 = 2, \ell = 0)$	$(v_6 = 1, \ell = 1)$
Number of levels	692	2177
$0.0 \leq \delta^{\star} \leq 2 \times 10^{-4} cm^{-1}$	86.8 %	86.2 %
$2 \times 10^{-4} \leq \delta^{\star} \leq 4 \times 10^{-4} cm^{-1}$	12.7 %	11.4 %
$4 \times 10^{-4} \leq \delta^{\star} \leq 6.2 \times 10^{-4} cm^{-1}$	0.4 %	2.4 %
Standard deviation (in cm^{-1})	0.14×10^{-3}	
(C) Microwave rotational transitions within the $(v_6 = 1, \ell = 1)$ and $(v_3 = 2, \ell = 0)$ vibrational states:		
$v_3 = 2$	$v_6 = 1$	both levels
95	160	255
0.0 MHz $\leq$ 92.63% $\leq$ 1.0 MHz	0.0 MHz $\leq$ 92.50% $\leq$ 1.0 MHz	0.0 MHz $\leq$ 92.55% $\leq$ 1.0 MHz
1.0 MHz $\leq$ 6.32% $\leq$ 2.0 MHz	1.0 MHz $\leq$ 7.50% $\leq$ 2.0MHz	1.0 MHz $\leq$ 7.06% $\leq$ 2.0MHz
2.0 $\leq$ 1.05% $\leq$ 4.0 MHz	2.0 MHz $\leq$ 0.00% $\leq$ 4.0 MHz	2.0 MHz $\leq$ 0.39% $\leq$ 4.0 MHz

* Pure "vibration-rotation" transitions and "hyperfine perturbed" subcomponents (see text).

⁎ Pure "vibration-rotation" transitions (see text).

* $\delta = |E_{obs} - E_{calc}|$.

▲ As an isolated state.

▼ As an isolated state.

♦ $(v_6 = 1, \ell = 1)$ accounting for $\alpha(\Delta\ell = \pm 1; \Delta K = \pm 2)$ and for $C_x(\Delta\ell = \pm 1; \Delta K = \pm 1)$ Coriolis resonance with $(v_2 = 1, \ell = 0)$ and $(v_3 = 2, \ell = 0)$ respectively.

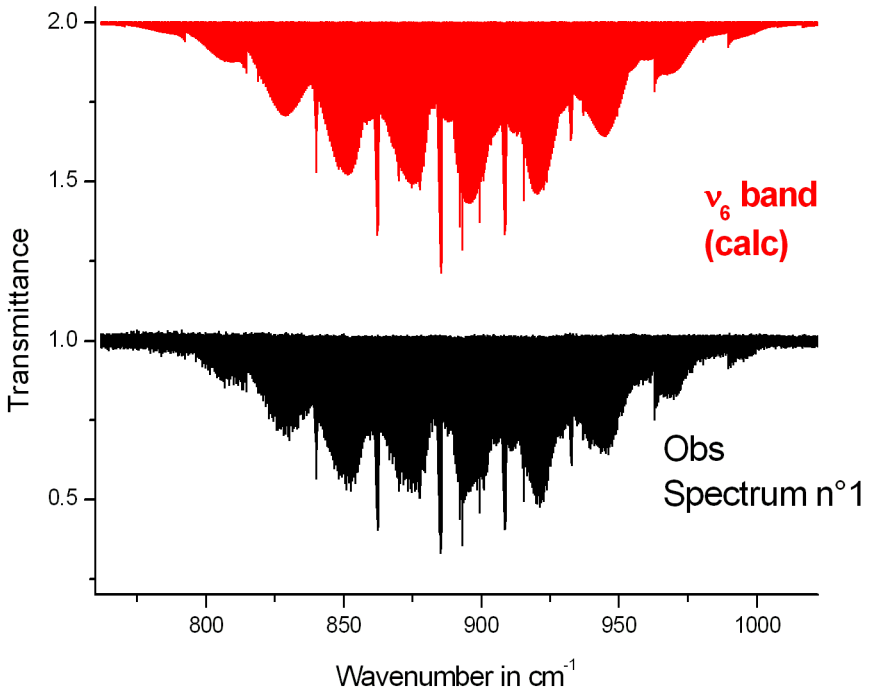

Figure 2: Overview of the absorption spectrum of $^{12}CH_3I$ (spectrum n°1) in the 740-1055 cm^{-1} spectral region. "Obs" trace: observed "spectrum n°1" recorded with a resolution of 1.02×10^{-3} cm^{-1}, an optical path length of 4 m, a pressure of 0.206 mbar and a stabilized temperature of 295 K. "Calc" trace: synthetic spectra, calculated for the ν_6 and $2\nu_3$ bands at the same experimental conditions using the line lists generated in this work. The observed and synthetic spectra are in transmission and shifted for clarity.

215

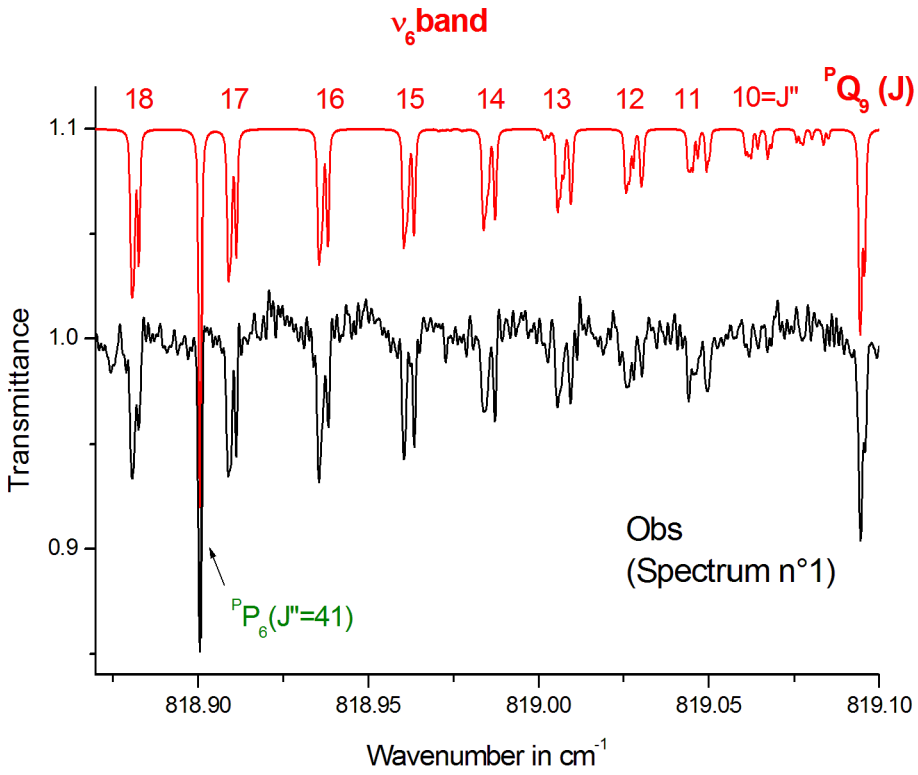

Figure 3: Portion of the absorption spectrum of $^{12}CH_3I$ (spectrum n°1) in the 818 cm^{-1} spectral region. The observed and synthetic spectra are in transmission and are shifted for the sake of clarity. Some assignments are given. For the $^{P}Q_9$ band-head, the hyperfine structure has to be accounted for.

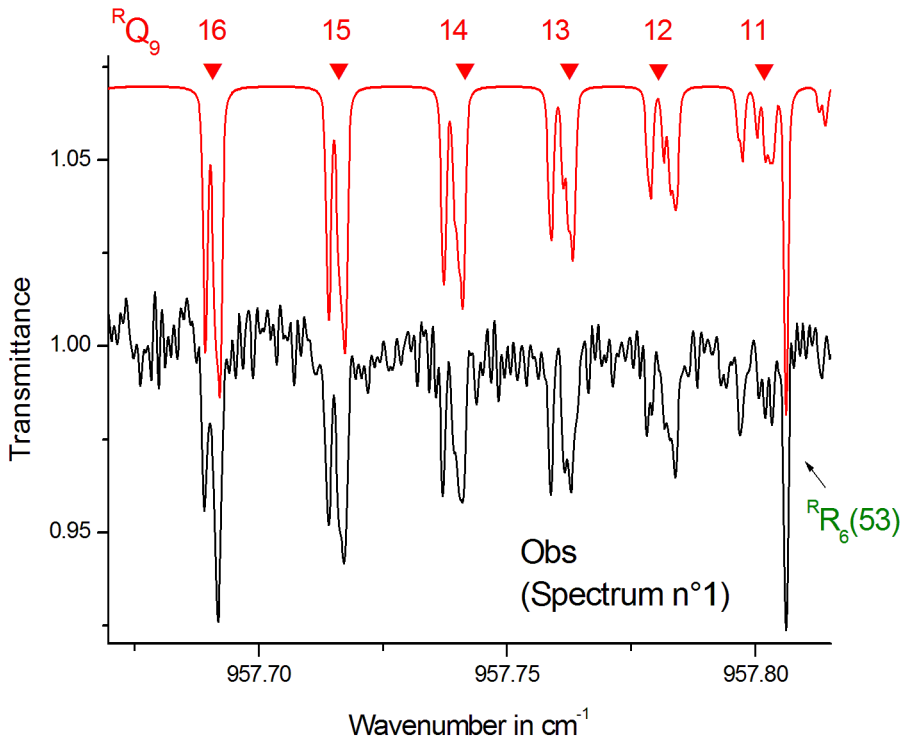

Figure 4: Portion of the absorption spectrum of $^{12}CH_3I$ (spectrum n°1) in the 957.7 cm^{-1} spectral region. The observed and synthetic spectra are in transmission and are shifted for the sake of clarity. Some assignments are given. For the $^{R}Q_9$ band-head, the hyperfine structure has to be accounted for.

4. Energy levels calculations

The infrared energy levels, achieved during the present study, were included in a least squares fit calculation together with the rotational transitions available in the literature, within the $v_6 = 1$ [4, 5, 1, 2] and the $v_3 = 2$ [1] vibrational states, which were achieved through different microwave techniques. Each set of data were accounted for at their estimated accuracy in a process which is

described in details in Reference [2]. The model used during this calculation is described in Appendix A. The hyperfine structure is accounted for during the computation of the rotational transitions within $v_6 = 1$ and $v_3 = 2$ states. As pointed out previously, it proved unnecessary to refine the electric quadrupole and spin-rotation parameters which were fixed to the values given in references [2] and [1] for $v_6 = 1$ and $v_3 = 2$, respectively.

Two types of energy levels calculations were performed. During our first two calculations, calculation n^o 1 and calculation n^o 2, we assumed that the $v_3 = 2$ and $v_6 = 1$ states can be considered as isolated ones, with no significant perturbation. As far as the $v_3 = 2$ state is concerned, it proved that we were not able to improve significantly the quality of the calculation, for the energy levels and for the microwave transitions, and this in comparison to the calculations previously perfomed by Alanko et al. [18] and by Wlodarczak et al. [1]. Therefore, the parameters quoted in table 4 are those given by Alanko et al. [18], and we accomplished a simple readjustment of the $v_3 = 2$ rotational parameters, and this is due to the fact that we used a different set of ground sate parameters [33] in respect to the one used by Alanko et al. [18]. On the other hand, during the calculation n^o 2, we had to refine significantly the $v_6 = 1$ parameters in order to reproduce the observed energy levels. The resulting parameters together with their associated uncertainties are collected in table 4 in the case $v_6 = 1$ state. This table compares the values obtained during the present work with the parameters achieved during the study conducted by Carocci et al. [2]. In comparison to this previous investigations [2] we considered one additional flexible parameter (η_{JKK}) during the energy level calculation. This was expected, since the present range of rotational energy levels exceeds the one achieved during these previous investigations. In the case of the infrared levels, the table 3 gives a statistical analysis of the (observed - calculated) values. It seems relevant to compare the quality of the present energy calculation with the one achieved when using the parameters (band centers and rotational constants) from references [2, 18]. This is not the case for the $v_6 = 1$ state, and figure 8 shows a plot of the Obs-Calc differences for the $v_6 = 1$ energy levels

as a function of the K and J rotational quantum numbers ($K + (J/100)$ in our case). It is clear that the centrifugal distortion constants are more reliable in the present work than in the reference [2] because we used a significantly larger set of energy levels. However, it is clear also that some series of energy levels could not be reproduce correctly. For example for the energy levels involving $(\ell \times k)$ =-17, the disagreement grows up with J to reach -1.7×10^{-3} cm^{-1} for $J = 37$. Therefore, it was clear that resonances due to other vibrational states may occur. According to the recommendation given by Paso and Alanko [16] we first performed a new calculation accounting for the $(\Delta\ell\ ;\ \Delta K) = (\pm 1;\ \pm 1)$ Coriolis resonance coupling the energy levels from $v_6 = 1$ with those of the $v_3 = 2$ state. We observe some progress in the quality of our fit, but still, the series of energy levels in $(\ell \times k)$ =-17 were not reproduced satisfactorily. We presumed that some series belonging to the $v_2 = 1$, ($v_3 = 1$;$v_6 = 1$) or $v_5 = 1$ states of $^{12}CH_3I$ [11] could possibly be involved in this resonance. After trials and errors, it appeared that the $v_2 = 1$ state was responsible for this resonance through an $\alpha(\Delta l = \pm 1; \Delta K = \pm 2)$ type Coriolis resonance. Therefore, in the final performed calculation we took into account the resonances involving the $v_6 = 1$ energy levels with those from both $v_3 = 2$ and $v_2 = 1$ levels. For the $v_2 = 1$ vibrational state, the band center and the ($^{v=2}$X-$^{v=0}$X) vibrational dependences of the rotational constants were maintained to the values proposed by Alanko [11]. The final set of band centers, rotational and interaction constants are given in table 4 together with their associated uncertainties. It is important to mention that for the $\alpha(\Delta l = \pm 1; \Delta K = \pm 2)$ resonance, only the second order term, $^{6,2}\alpha_K$, could be determined. We presume that this is due to the fact that our calculation does not account for the resonances which couple together the $v_2 = 1$ energy levels with those of the ($v_3 = 1$;$v_6 = 1$) and $v_5 = 1$ states. These resonances are rather weak. To give an order of magnitude, the percentage of mixing of the wave-functions for the following resonating series are, for $J = 75$:

- $v_6 = 1, (\ell \times K) = -17 \Leftrightarrow v_2 = 1, K = 15$: mixing of 0.5 %
- $v_6 = 1, (\ell \times K) = +18 \Leftrightarrow v_2 = 1, K = 16$: mixing of 0.5 %

- $v_6 = 1, (\ell \times K) = +20 \Leftrightarrow v_3 = 2, K = 19$: mixing of 0.6 %
- $v_6 = 1, (\ell \times K) = +19 \Leftrightarrow v_3 = 2, K = 18$: mixing of 0.1 %

However, provided that the analysis is pursued up to rather high values of the rotational quantum numbers, even for the lower energy vibrational state, it proved that the $v_6 = 1$ level of $^{12}CH_3I$ cannot be considered as a true "isolated" state because its higher energy levels are coupled with those from other states, $v_3 = 2$ and $v_2 = 1$. Such situation occurs for many molecules, particularly in the case of $^{12}CH_3F$ [34] and HDCO [35], for example. Table 3 gives a statistical analysis on the results of this energy level calculation (Calculation n^o 3). In figure 8, the Obs-Calc differences, in energy, are plotted as a function of the rotational quantum numbers $(K + (J/100))$. It is clear that the progress is significant, especially for the series in $(\ell \times K)$=15 and in $(\ell \times K)$ =-17. Finally, the (C) part of table 3 describes the results of the present calculation concerning the data existing in the literature for the rotational transitions within the $v_6 = 1$ and $v_3 = 2$ vibrational states. There is no significant differences in term of quality of the fit between the two types of computations (calculations n^o 1 and n^o 2 and calculation n^o 3). Furthermore, these results in case of the microwave data are also quite similar in quality to those achieved previously in the literature when using the previous set of vibrational energies, rotational and hyperfine constants [2, 18, 1].

To check the quality of our calculation, a line list in positions and relative intensities was generated for the v_6 and $2v_3$ bands. Therefore, we used the vibration-rotation parameters quoted in table 4 for the computation of the $v_6 = 1$ and $v_3 = 2$ rotation energy levels, and the rotation constants of reference [2] in the case of the ground state. The hyperfine structure of the lines was accounted for by using the hyperfine parameters quoted in table 4 [2, 1]. The relative line intensities were computed as described previously.

Figures 2 and 5 give overviews of the v_6 and $2v_3$ bands while figures 3, 4, 6 and 7 compare the observed and calculated spectra in several regions of these bands. It is clear that the agreement is very satisfactorily for v_6 lines even when

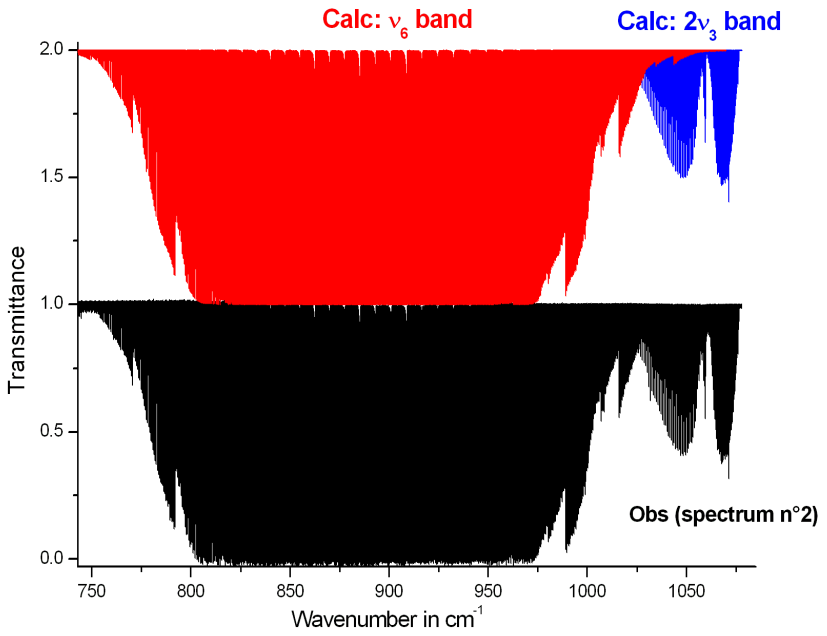

Figure 5: Overview of the absorption spectrum of $^{12}CH_3I$ (spectrum n°2) in the 740-1020 cm^{-1} spectral region. "Obs" trace: observed "spectrum n°2" recorded with a resolution of 0.0019 cm^{-1}, an optical path length of 4 m, a pressure of 0??0.34 mbar and a stabilized temperature of 293 K. "Calc " trace: synthetic spectra, calculated for the v_6 band at the same experimental conditions using the line lists generated in this work. The observed and synthetic spectra are in transmission and shifted for clarity.

the hyperfine structure is quite observable (figures 3,4 and 6). The agreement is as well satisfactory for v_6 transitions involving high K values and for $2v_3$ transitions (figure 7).

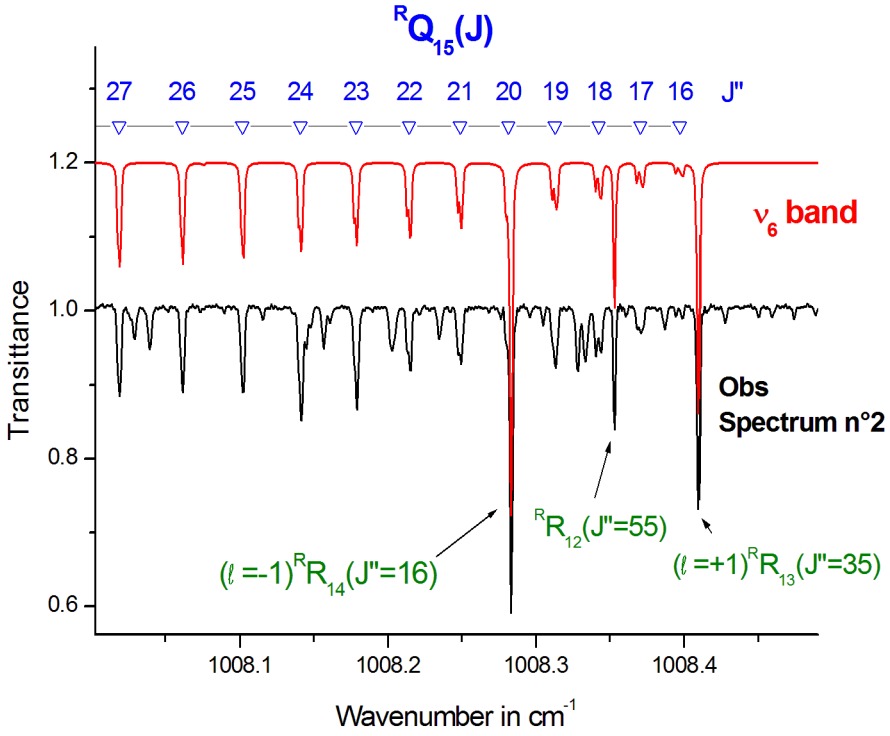

Figure 6: Portion of the absorption spectrum of $^{12}CH_3I$ (spectrum n°2) in the 1008.3 cm^{-1} spectral region (spectrum "2"). The observed and synthetic spectra are in transmission and shifted for clarity. Some assignments are given. For the $^{R}Q_15$ band-head, the hyperfine structure has to be accounted for.

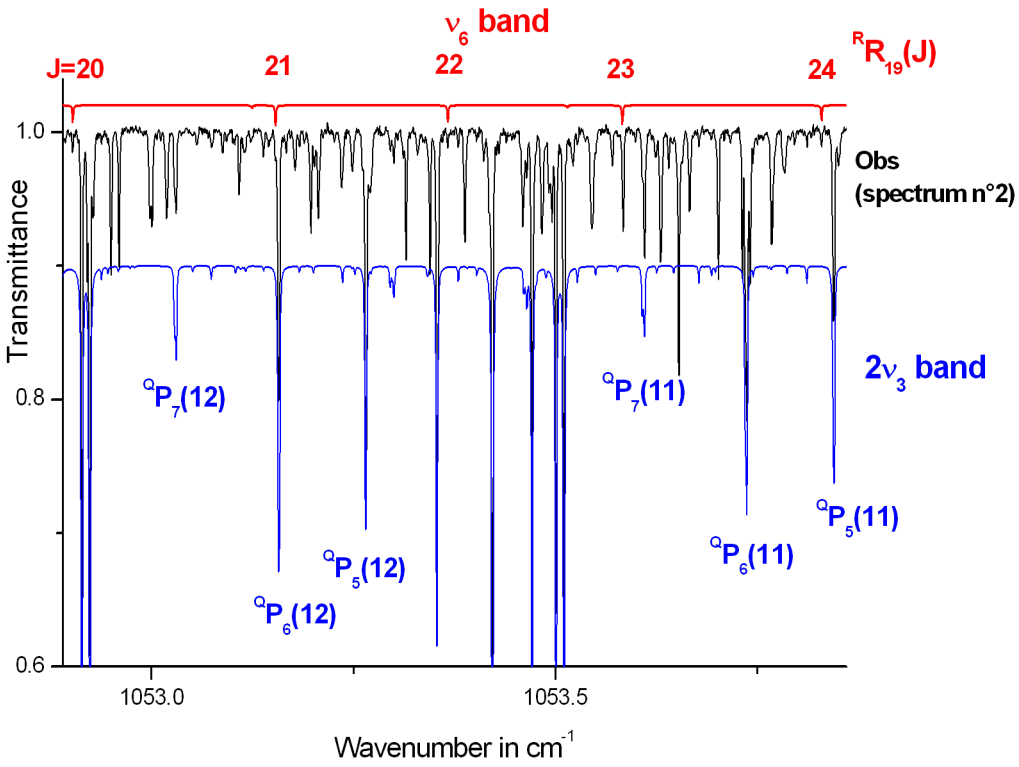

Figure 7: Portion of the absorption spectrum of $^{12}CH_3I$ (spectrum n°2) in the 1053.5 cm^{-1} spectral region (spectrum "2"). The observed and synthetic spectra are in transmission and shifted for clarity. Some assignments are given for the $2v_3$ bands, together with lines from the v_6 band involving high $K = 20$ in the upper energy levels.

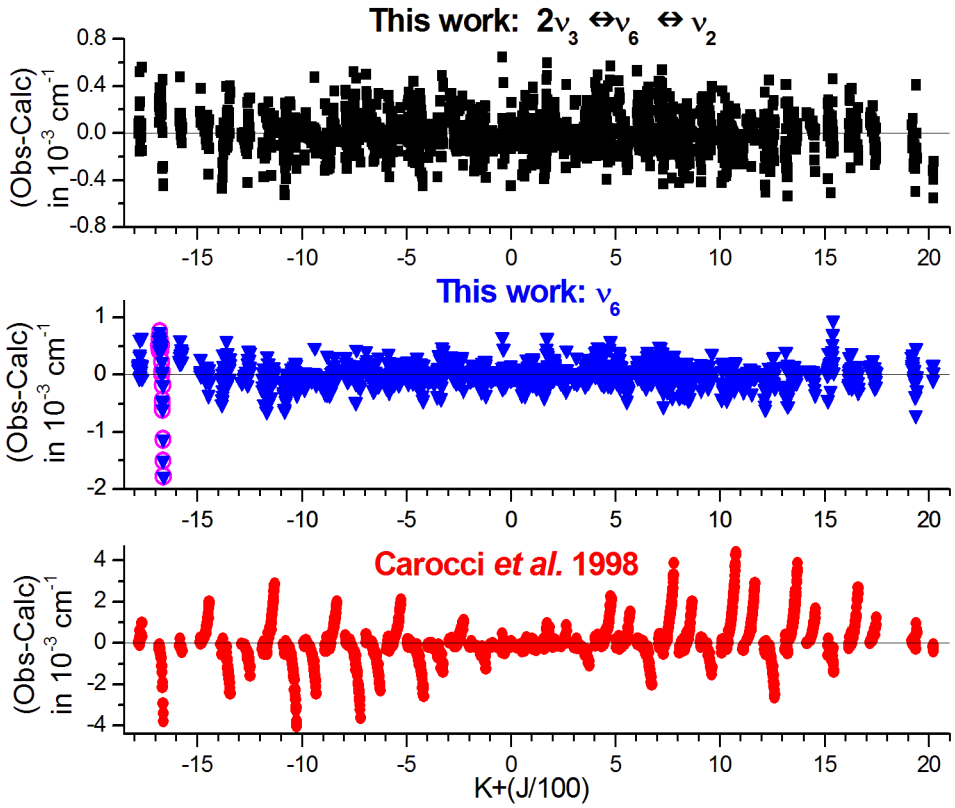

Figure 8: Plots of the (observed- calculated) energy levels for the $v_6 = 1$ as a function of $[(\ell \times K) + J/100]$ and this for different sets of $v_6 = 1$ parameters (band centers, rotational and coupling constants). Note the difference of scale in the y-axes for the three traces. Lower trace: $v_6 = 1$ as an isolated state and the parameters of reference [2]. Medium trace : $v_6 = 1$ as an isolated state and the parameters are taken from the table 4 of this work (calculation n^o 1). Noticeable disagreements are obtained for energy levels involving $K = -17$ (open circles). Upper trace: $v_6 = 1$ in resonance with $v_2 = 1$ and $v_3 = 2$ and the parameters from table 4 of this work (calculation n^{o}3).

Table 3: Vibrational and rotational constants for the ground and the $v_3 = 2$ vibrational states (Calculation n^o 1).

		Calculation n^o 1
	Ground	($v_3 = 2, \ell = 0$)
	[2]	[18]*
E_v (cm^{-1})		1059.993378
A (GHz)	155.1106938	154.703709
B (GHz)	7.501275753	7.39248335
D_J (kHz)	6.30762	6.392491
D_{JK} (kHz)	98.7657	98.6572
D_K (MHz)	2.62714	2.594741
H_J (mHz)	-3.431	[a]
H_{JK} (mHz)	58.8	[a]
H_{KJ} (Hz)	4.602	[a]
H_K (Hz)	135.6	[a]

[a] Fixed to the ground state value [2].

* Calculated from the ground state parameters of reference [2] and the (X''-X') $2\nu_3$ vibrational dependence of the rotational constants.

Table 4: Hyperfine constants for the ground and the ($v_6 = 1, \ell = 1$) and ($v_3 = 2, \ell = 0$) vibrational states of CH_3I.

	Ground [a]	($v_6 = 1, \ell = 1$) [a]	($v_3 = 2, \ell = 0$) [b]
eqQ (GHz)	-1.9341306	-1.94034	1.93478
X_J (kHz)	-1.55	-1.81	
X_K (kHz)	-33.36	-37.6	
X_d (kHz)	22.45	20.83	
η (kHz)		-1.19	
C_N ($\times 10^{-3}$)	-17.398	17.62	-13.92
C_K (kHz)	-17.10	-28.53	

[a] Reference [2].

[b] Reference [1].

Table 5: Vibrational energies, rotational and centrifugal distortion constants for the ($v_6 = 1, \ell = 1$) Considered as an isolated state.

	$v_6 = 1$	
	This work (calc. n° 2)	Reference [2]
E_v (cm^{-1})	882.918 38 (1)	882.918 206 4 (6)
(A_ζ)(GHz)	32.852 43 (32)	32.852 482 (22)
η_J(kHz)	200.899 (41)	200.933 (33)
η_K(MHz)	4.153 6 (11)	4.161 92 (76)
η_{JJ}(mHz)	159.4 (68)	157.4 (86)
η_{JK}(Hz)	9.30 (63)	9.04 (24)
η_{KK}(Hz)	-760.4 (40)	-792.8 (32)
η_{JKK}(mHz)	6.8 (26)	–
q_{22}^6 (MHz)	-1.480 52 (14)	-1.480 5 (13)
$q_{22}^{6,J}$ (Hz)	4.515 (42)	4.513 (32)
A (GHz)	156.150 901 1 (11)	156.150 936 9(53)
B (GHz)	7.477 662 25 (24)	7.477 663 12 (22)
D_J (kHz)	6.349 61 (14)	6.349 91 (18)
D_{JK} (kHz)	98.799 7 (61)	98.825 6 (45)
D_K (MHz)	2.729 30 (10)	2.729 748 (55)
H_J (mHz)	-3.715 (18)	-3.697 (34)
H_{JK} (mHz)	68.33 (98)	69.2 (28)
H_{KJ} (Hz)	3.824 (26)	4.010 (27)
H_K (Hz)	141.58 (25)	143.14 (18)

Table 6: Vibrational and rotational constants for the $v_2 = 1$, $v_3 = 2$, and $v_6 = 1$ interacting vibrational states of $^{12}CH_3I$.

	calculation n° 3		
	$v_2 = 1$	$v_6 = 1$	$v_3 = 2$
E_v (cm^{-1})	125 1.192 826*	882.918 37 (1)	105 9.993 58 (3)
(A_ζ)(GHz)		32.852 519 (41)	
η_J(kHz)		201.009 (46)	
η_K(MHz)		4.159 6 (14)	
η_{JJ}(mHz)		166.9(79)	
η_{JK}(Hz)		8.87 (34)	
η_{KK}(Hz)		-775.97 (177)	
η_{JKK}(mHz)			
q_{22}^6 (MHz)		-1.479 68 (17)	
$q_{22}^{6,J}$ (Hz)		4.521 (48)	
A (GHz)	155.725 385**	156.150 947 (12)	154.703 776 (29)
B (GHz)	7.475 513 96**	7.477 664 07 (25)	7.392 479 45 (65)
D_J (kHz)	6.356 622**	6.349 66 (14)	6.392 48 (16)
D_{JK} (kHz)	99.387 5**	98.821 8 (61)	98.668 (10)
D_K (MHz)	2.712 53**	2.729 84 (11)	2.595 24 (19)
H_J (mHz)	a	-3.706 (19)	a
H_{JK} (mHz)	a	71.6 (10)	a
H_{KJ} (Hz)	a	4.109 (29)	a
H_K (Hz)	a	142.97 (28)	a
$^{33,6}C_x$ (MHz)		92.98(16)	
$^{2,6}\alpha_K$ (Hz)	9.01(41)		

[a] Fixed to the ground state value.

[*] Reference [11].

[**] Calculated from the ground state parameters of reference [2] and the (X''-X') ν_2 vibrational dependence of the rotational constants [11].

5. conclusion

During this work a new analysis of the v_6 and $2v_3$ bands was performed using high resolution Fourier transform spectra. Along the assignment process, the hyperfine structure was accounted for during the analysis procedure as well as during the energy level calculation. In consequence, a large set of experimental energy levels was accurately measured for the $v_6 = 1$ and the $v_3 = 2$ states. The energy levels calculation was performed by considering, in a preliminary step, the $v_6 = 1$ and the $v_3 = 2$ as an isolated states. In an advanced stage of the study, it proved necessary to account for the resonances which were found to couple the $v_6 = 1$ energy levels with those of $v_3 = 2$ and $v_2 = 1$.

6. Acknowledgements

The DECA-PF project, launched end of 2013 for 3 years, is sponsored by the French government 'Investments for the future' programme through the grant ANR-11-RSNR-0003 supervised by the French National Research Agency (ANR) under the 'Research in Nuclear Safety and Radioprotection' (RSNR) research initiative.

The authors are grateful to Dr. Jean Demaison for his kind advises during the process of this study and for a careful reading of the manuscript.

A. Appendix.

Table 7: Hamiltonian matrix used to describe the {($v_6 = 1$; $\ell = \pm 1$),($\nu_3 = 2$;$\ell = 0$),($v_2 = 1$;$\ell = 0$)} resonating states of CH_3I.

	($v_6 = 1$; $\ell = \pm 1$)	($v_3 = 2$;$\ell = 0$)	($v_2 = 1$;$\ell = 0$)
($v_6 = 1$; $\ell = \pm 1$)	${}^6W + {}^6 Hyp$	c.c.	c.c.
($v_3 = 2$;$\ell = 0$)	$C_x(\Delta\ell = \pm 1; \Delta K = \pm 1)$	${}^{33}W + {}^{33} Hyp$	
($v_2 = 1$;$\ell = 0$)	$\alpha(\Delta\ell = \pm 1; \Delta K = \pm 2)$		${}^2W + {}^2 Hyp$

(A) Vibrational rotational operators : The W(v; $\ell = \pm 1$) are rotational diagonal in v-operators, including both diagonal and non diagonal ℓ terms. The $(\Delta\ell; \Delta K)$ =(0; 0) z-type Coriolis and Anharmonic rotational operator.

(1) $W(\mathrm{v}; \ell = \pm 1)$ v-diagonal operators :

$\langle \mathrm{v}; \ell, JK | \mathcal{H} | v; \ell, JK \rangle = E_{\mathrm{v}} + B_{\mathrm{v}} J(J+1) + (A_{\mathrm{v}} - B_{\mathrm{v}}) K^2$

$- D_J^{\mathrm{v}} J^2(J+1)^2 - D_{JK}^{\mathrm{v}} K^2(J+1) - D_K^{\mathrm{v}} K^4 + H_J^{\mathrm{v}} J^3(J+1)^3$

$+ H_{JK}^{\mathrm{v}} J^2(J+1)^2 K^2 + H_{KJ}^{\mathrm{v}} J(J+1) K^4 + H_K^v K^6 + L_{KJ} K^4 J^2(J+1)^2$

$+ \left[-2A_{\varsigma v} + \eta_J^v J(J+1) + \eta_K^v K^2 + \eta_{JJ}^v J^2(J+1)^2 + \eta_{JK}^v K^2(J+1) + \eta_{JKK}^v K^4 J(J+1) \right] K\ell$

The diagonal z-Coriolis terms ($A_{\varsigma v}$) and their expansion (η^{v} ect..) vanish for all $\ell = 0$ vibrational states ($\nu_2 = 1$ and $\nu_3 = 2$).

For the ($\mathrm{v}_6 = 1$; $\ell = \pm 1$) vibrational state, the $(\Delta\ell; \Delta K) = (\pm 2; \pm 2)$ - type of operator was taken into account. [3]

$\langle \mathrm{v}; \ell = \pm 1, JK | \mathrm{H} | \mathrm{v}; \ell = \pm 1, JK \pm 2 \rangle =$

$2 \left(\mathrm{q}_{22}^{\mathrm{v}} + q_{22}^{\mathrm{v},J} J(J+1) \right) \times F_2(J, K, K \pm 1)$

(2) C($\pm 1; \pm 1$) Coriolis off diagonal in v operator.[4]

$\langle \mathrm{v}_6 = 1; \ell = \pm 1, JK | \mathrm{H} | \mathrm{v}_2 = 1; \ell = 0, JK \pm 2 \rangle =$

$\pm \left({}^{6,2}\alpha_0 + {}^{6,2}\alpha_K \left(K^2 + (K \pm 2)^2 \right) \right) F_2(J, K, K \pm 2)$

$\langle \mathrm{v}_6 = 1; \ell = \pm 1, JK | \mathrm{H} | \mathrm{v}_3 = 2; \ell = 0, JK \pm 1 \rangle = {}^{6,33}C_0 F_1(J, K, K \pm 1)$

$F_2(J, K, K \pm 2) = \sqrt{J(J+1) - (K(K \pm 1))(J(J+1)) - (K \pm 1)(K \pm 2)}$

$F_1(J, K, K \pm 2) = \sqrt{J(J+1) - K(K \pm 1)}$

(B) Hyperfine operators (Hyp(v)): For CH_3I, two type of hyperfine operators are to be considered in order to describe the observed hyperfine structure:

1. The nuclear quadrupole operator H_{Quadr}:

   - Diagonal term :

     $\langle J, K, F | H_{Quadr} | J, K, F \rangle =$

[3] Note the different convention used in reference [2] for the $(\Delta\ell; \Delta K) = (\pm 2; \pm 2)$ off-diagonal operator and as a consequence for the q_{22}^{WW} parameter :

$\langle \mathrm{v}; \ell = \pm 1, JK | \mathrm{H} | \mathrm{v}; \ell = \pm 1, JK \pm 2 \rangle = 1/2 F_2(J, K, K \pm 2) \times (q_{22}^{WW} + ...)$

[4] The $\alpha(\Delta\ell = \pm 1; \Delta K = \pm 2)$ Coriolis operator is set at zero when the Coriolis resonances are not considered explicitly.

$$(eqQ'' + X''_J J(J+1) + X''_K K^2) \times \left(\frac{3K^2}{J(J+1)} - 1\right) + X''_d \frac{K^2(4K^2-1)}{J(J+1)}\, Y(I,J,F)$$

where;

$$Y(I,J,F) = \frac{3C(C+1) - I(I+1)J(J+1)}{8I(2I-1)(2J-1)(2J+3)}$$

where;

$$C = F(F+1) - I(I+1) - J(J+1)$$

- Non diagonal terms :

$$\langle J,K,F|\, H_{Quadr}\, |J+1,K,F\rangle = \frac{3eqQ''K\,[F(F+1) - I(I+1) - J(J+2)]}{8I(2I-1)J(J+2)}$$

$$\times \left[\left(1 - \frac{K^2}{(J+1)^2}\right)(I+J+F+2) \times \frac{(J+F-I+1)(I+F-J)(I+J-F+1)}{(2J+1)(2J+3)}\right]\frac{1}{2}$$

and;

$$\langle J,K,F|\, H_{Quadr}\, |J+2,K,F\rangle = \frac{3eqQ''}{16I(2I-1)(2J+3)}$$

$$\times \left[(1 - \frac{K^2}{J^2(J+1)^2})(1 - \frac{K^2}{J^2(J+2)^2})(I+J+F+3)\right.$$

$$\times (I+J+F+2)(I+J-F+2)(I+J-F+1)(J+F-I+2)$$

$$\left.\times \frac{(J+F-I+1)(I-J+F)(I+F-J-1)}{(2J+1)(2J+5)}\,\frac{1}{2}\right.$$

2. The spin- rotation operator H_{SR}:

$$H_{SR} = -\frac{1}{2}\left[C''_N + (C''_K - C''_N)\frac{K^2}{J(J+1)}\right] \times F(F+1) - I(I+1) - J(J+1)$$

References

[1] G. Wlodarczak, D. Boucher, R. Bocquet, J. Demaison, The rotational constants of methyl lodide, Journal of Molecular Spectroscopy 124 (1) (1987) 53 – 65. doi:http://dx.doi.org/10.1016/0022-2852(87)90120-2. URL http://www.sciencedirect.com/science/article/pii/0022285287901202

[2] S. Carocci, A. D. Lieto, A. D. Fanis, P. Minguzzi, S. Alanko, J. Pietil, The molecular constants of $^{12}CH_3I$ in the ground and $v_6 = 1$ excited vibrational state, Journal of Molecular Spectroscopy 191 (2) (1998) 368 –

373. doi:http://dx.doi.org/10.1006/jmsp.1998.7652.
URL http://www.sciencedirect.com/science/article/pii/S0022285298976524

[3] N. Bell, L. Hsu, D. J. Jacob, M. G. Schultz, D. R. Blake, J. H. Butler, D. B. King, J. M. Lobert, E. Maier-Reimer, Methyl iodide: Atmospheric budget and use as a tracer of marine convection in global models, Journal of Geophysical Research: Atmospheres 107 (D17) (2002) ACH 8–1–ACH 8–12, 4340. doi:10.1029/2001JD001151.
URL http://dx.doi.org/10.1029/2001JD001151

[4] Radio-frequency spectroscopy inside a laser cavity;.

[5] A. Dubrulle, J. Burie, D. Boucher, F. Herlemont, J. Demaison, Microwave spectra of methyl chloride, methyl bromide, and methyl iodide in the $v_6 =$ 1excited vibrational state, Journal of Molecular Spectroscopy 88 (2) (1981) 394 – 401. doi:http://dx.doi.org/10.1016/0022-2852(81)90189-2.
URL http://www.sciencedirect.com/science/article/pii/0022285281901892

[6] S. Belli, G. Buffa, A. Di Lieto, P. Minguzzi, O. Tarrini, M. Tonelli, Hyperfine level dependence of the pressure broadening of CH_3I rotational transitions in the $v_6 = 1$ vibrational state, Journal of Molecular Spectroscopy 201 (2) (2000) 314 – 318. doi:http://dx.doi.org/10.1006/jmsp.2000.8106.
URL http://www.sciencedirect.com/science/article/pii/S0022285200981062

[7] R. Paso, V.-M. Horneman, R. Anttila, Analysis of the v_1 band of CH_3I, Journal of Molecular Spectroscopy 101 (1) (1983) 193 – 198. doi:http://dx.doi.org/10.1016/0022-2852(83)90017-6.
URL http://www.sciencedirect.com/science/article/pii/0022285283900176

[8] S. Alanko, V.-M. Horneman, J. Kauppinen, The v_3 band of CH_3I around 533 cm^1, Journal of Molecular Spectroscopy 135 (1) (1989) 76 – 83. doi:http://dx.doi.org/10.1016/0022-2852(89)90355-X.
URL http://www.sciencedirect.com/science/article/pii/002228528990355X

[9] R. Anttila, R. Paso, G. Guelachvili, A high-resolution infrared study of the v_4 band of CH_3I, Journal of Molecular Spectroscopy 119 (1) (1986) 190 – 200. doi:http://dx.doi.org/10.1016/0022-2852(86)90213-4.
URL http://www.sciencedirect.com/science/article/pii/0022285286902134

[10] Y. Zhao, Z. Shen, Q. Zhu, C. Zhang, A complete least-squares analysis of a high-resolution laser spectroscopic study of CH_3I v_5 fundamental, Journal of Molecular Spectroscopy 115 (1986) 34 – 46. doi:http://dx.doi.org/10.1016/0022-2852(86)90273-0.
URL http://www.sciencedirect.com/science/article/pii/0022285286902730

[11] S. Alanko, A detailed analysis of the $v_2/v_5/v_3+v_6$ band system of $^{13}CH_3I$ and $^{12}CH_3I$, Journal of Molecular Spectroscopy 177 (2) (1996) 263 – 279. doi:http://dx.doi.org/10.1006/jmsp.1996.0140.
URL http://www.sciencedirect.com/science/article/pii/S002228529690140X

[12] H. Matsuura, J. Overend, Infrared spectra of ch3i, the n6 and n2+n6 bands, Spectrochimica Acta 27A.

[13] P. P. Das, V. M. Devi, K. N. Rao, Diode laser spectroscopy of the v_6 band of $^{12}CH_3I$, Journal of Molecular Spectroscopy 84 (1) (1980) 305 – 312. doi:http://dx.doi.org/10.1016/0022-2852(80)90261-1.
URL http://www.sciencedirect.com/science/article/pii/0022285280902611

[14] H.-J. Clar, M. Reich, R. Schieder, G. Winnewisser, K. M. Yamada, Diode laser spectrum of the v_6 band of CH_3I using a novel étalon as a calibration scale, Journal of Molecular Spectroscopy 112 (2) (1985) 447 – 458. doi:http://dx.doi.org/10.1016/0022-2852(85)90175-4.
URL http://www.sciencedirect.com/science/article/pii/0022285285901754

[15] S. Alanko, The v_6 band of $^{13}CH_3I$, Journal of Molecular Spectroscopy 147 (2) (1991) 406 – 413. doi:http://dx.doi.org/10.1016/0022-2852(91)90066-J.
URL http://www.sciencedirect.com/science/article/pii/002228529190066J

[16] R. Paso, S. Alanko, The effect of nuclear quadrupole hyperfine interaction on the infrared absorption band ν_6 of $^{12}CH_3I$, Journal of Molecular Spectroscopy 157 (1) (1993) 122 – 131. doi:http://dx.doi.org/10.1006/jmsp.1993.1010.
URL http://www.sciencedirect.com/science/article/pii/S0022285283710106

[17] I. Haykal, D. Doizi, V. Boudon, A. El Hilali, L. Manceron, G. Ducros, Line positions in the $v_6 = 1$ band of methyl iodide: validation of the C_{3v}TDS package based on the tensorial formalism, Journal of Quantitative Spectroscopy and Radiative Transfer 173 (2016) 13 – 19. doi:http://dx.doi.org/10.1016/j.jqsrt.2015.12.016.
URL http://www.sciencedirect.com/science/article/pii/S0022407315302090

[18] S. Alanko, V.-M. Horneman, R. Anttila, R. Paso, Overtone bands $2v_3$ of $^{12}CH_3I$ and $^{13}CH_3I$, Journal of Molecular Spectroscopy 141 (1) (1990) 149 – 166. doi:http://dx.doi.org/10.1016/0022-2852(90)90285-X.
URL http://www.sciencedirect.com/science/article/pii/002228529090285X

[19] F. Lattanzi, Parallel vibrational states of CH_3I in the high resolution infrared spectrum from 2770 to 2900 cm1, The Journal of Chemical Physics 92 (7).

[20] T. Sullivan, L. Frenkel, Measurement of fourth order distortion constants in symmetric top molecules, Journal of Molecular Spectroscopy 39 (2) (1971) 185 – 201. doi:http://dx.doi.org/10.1016/0022-2852(71)90052-X.
URL http://www.sciencedirect.com/science/article/pii/002228527190052X

[21] D. Boucher, J. Burie, D. Dangoisse, J. Demaison, A. Dubrulle, Doppler-free rotational spectrum of methyl iodide. nuclear quadrupole, spin-rotation and nuclear shielding tensors of iodine, Chemical Physics 29 (3) (1978) 323 – 330. doi:http://dx.doi.org/10.1016/0301-0104(78)85082-4.
URL http://www.sciencedirect.com/science/article/pii/0301010478850824

[22] S. Young, S. Kukolich, Microwave measurements and calculations of quadrupole coupling effects in CH_3I and CD_3I, Journal of Molecular Spectroscopy 114 (2) (1985) 483 – 493. doi:http://dx.doi.org/10.1016/0022-2852(85)90240-1.
URL http://www.sciencedirect.com/science/article/pii/0022285285902401

[23] B. Osipov, M. N. Grabois, Magnetic hyperfine structure and centrifugal distortion in quadrupole spectra of $^{12}CH_3I$ and $^{13}CH_3I$, Journal of Molecular Spectroscopy 111 (2) (1985) 344 – 351. doi:http://dx.doi.org/10.1016/0022-2852(85)90010-4.
URL http://www.sciencedirect.com/science/article/pii/0022285285900104

[24] C. Wenger, V. Boudon, M. Rotger, M. Sanzharov, J.-P. Champion, XTDS and SPVIEW: Graphical tools for the analysis and simulation of high-

resolution molecular spectra, Journal of Molecular Spectroscopy 251 (12) (2008) 102 – 113.

[25] A. El Hilali, V. Boudon, M. Loëte, Spectroscopy of XY_3Z (C_{3v}) molecules: A tensorial formalism adapted to the $O(3) \supset C_{\infty v} \supset C_{3v}$ group chain, J. Mol. Spec. 234 (2005) 113–121.

[26] R. Paso, R. Anttila, G. Guelachvili, Perturbations in the v_1 band of CH_3I, Journal of Molecular Spectroscopy 140 (1) (1990) 46 – 53. doi:http://dx.doi.org/10.1016/0022-2852(90)90005-B.
URL http://www.sciencedirect.com/science/article/pii/002228529090005B

[27] F. Mbay, L. Manceron, Article in preparation.

[28] J. E. Dickens, W. M. Irvine, M. Ohishi, M. Ikeda, S. Ishikawa, A. Nummelin, . Hjalmarson, Detection of interstellar ethylene oxide (c-c_2h_4o), The Astrophysical Journal 489 (2) (1997) 753.
URL http://stacks.iop.org/0004-637X/489/i=2/a=753

[29] C. Bray, A. Perrin, D. Jacquemart, N. Lacome, The v_1, v_4 and $3v_6$ bands of methyl chloride in the 3.4-μm region: Line positions and intensities, Journal of Quantitative Spectroscopy and Radiative Transfer 112 (15) (2011) 2446 – 2462. doi:http://dx.doi.org/10.1016/j.jqsrt.2011.06.018.
URL http://www.sciencedirect.com/science/article/pii/S0022407311002305

[30] G. Tarrago, M. Delaveau, Triad $v_n(a_1)$, $v_t(e)$, $v_t^{'}(e)$ in C_{3v} molecules: Energy and intensity formulation (computer programs), Journal of Molecular Spectroscopy 119 (2) (1986) 418 – 425. doi:http://dx.doi.org/10.1016/0022-2852(86)90036-6.
URL http://www.sciencedirect.com/science/article/pii/0022285286900366

[31] I. Bowater, J. Brown, A. Carrington.

[32] W. Gordy, R. L. Cook, Microwave molecular spectra / Walter Gordy, Robert L. Cook, 3rd Edition, Wiley New York, 1984.

[33] S. Carocci, A. D. Lieto, A. Menciassi, P. Minguzzi, M. Tonelli, High-resolution rotational spectroscopy of CH_3I using a novel doppler-free technique, Journal of Molecular Spectroscopy 175 (1) (1996) 62 – 67. doi:http://dx.doi.org/10.1006/jmsp.1996.0009.
URL http://www.sciencedirect.com/science/article/pii/S0022285296900090

[34] D. Papoušek, P. Pracna, M. Winnewisser, S. Klee, J. Demaison, Simultaneous rovibrational analysis of the v_2, v_3, v_5, and v_6 bands of $^{12}CH_3F$, Journal of Molecular Spectroscopy 196 (2) (1999) 319 – 323. doi:http://dx.doi.org/10.1006/jmsp.1999.7875.
URL http://www.sciencedirect.com/science/article/pii/S002228529997875X

[35] L. Gomez, A. Perrin, G. Mellau, New analysis of the v_3 fundamental band of hdco: Positions and intensities, Journal of Molecular Spectroscopy 256 (1) (2009) 28 – 34, pRAHA2008, The 20th International Conference on High Resolution Molecular Spectroscopy. doi:http://dx.doi.org/10.1016/j.jms.2009.01.010.
URL http://www.sciencedirect.com/science/article/pii/S0022285209000125